TECHNICAL REPORT No. 45

THE EFFECT OF MECHANICAL FORCING ON THE FORMATION OF A MESOSCALE VORTEX

by

Guo-xiong Wu* and Shou-jun Chen**

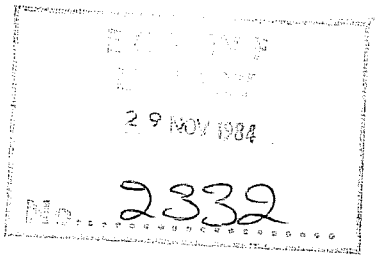

* Visiting scientist on leave from
Institute of Atmospherics Physics,
Academia Sinica, Beijing, China.

** Visiting scientist on leave from
Department of Geophysics,
Beijing University, Beijing, China.

October 1984

ABSTRACT

The influence of mechanical forcing on the formation of a mesoscale vortex which occurred over the eastern flank of the Qinghai-Tibetan Plateau (QTP) is investigated by running a series of numerical experiments. Different orography schemes are tested. It is shown that there are three branches of air flow converging towards the vortex: the northerlies associated with the middle latitude westerly currents, the southerlies with the low-level monsoon jet, and the easterlies with the West Pacific Subtropical High. These flows are very sensitive to mechanical forcing and play very important roles in the formation and location of the vortex.

The model with either the mean or the envelope orography is shown to be capable of predicting the formation of the vortex and the associated torrential rain. However, its location is not predicted precisely. A modified orography, simulating the "step" structure of the eastern flank of the QTP, is then used in an attempt to improve the prediction. Results from this experiment show that the weakening of some of the steep slopes of the large-scale orography in a numerical model, due to excessive smoothing of mountain height and expanding of mountain area, is responsible for the inaccuracy in the forecast of such synoptic systems. Therefore further improvements in the orography scheme are discussed.

C O N T E N T S

1. INTRODUCTION

During the Asian monsoon period, torrential rain which occurs over the northeast flank of the Qinghai-Tibetan Plateau (QTP) develops so rapidly and intensely that its prediction based on synoptic meteorology appears to be very difficult, and severe casualties can result. Despite many efforts on, and contributions to, the study of the generation and prediction of such torrential rain, the mechanisms which cause them are still not very clear.

Generally speaking, two categories of weather situations are favourable for such torrential rain to occur over that area. One is the confluence flow associated with frontogenesis, and the other is the mesoscale-α vortex or shear-line (as defined by Orlansky, 1975). The first category occurs when an eastward propagating cold mid-latitude westerly trough approaches the warm West Pacific Subtropical High (WPSH). The confluent flow at 500 mb is then composed of the southwesterlies, in front of the westerly trough, and the southerlies or south-southwesterlies, west of the WPSH (Wu, 1977). The cold advection from the west and the warm advection from the south thus produce a region favourable for cyclogenesis. By writing the guasi-geostrophic ω-equation in the natural coordinates, Wu (1978) investigated the vertical motions in such a field and found that, on the right hand side of the entrance of this confluent flow, the geostrophic balance between the wind and geopotential fields, and the hydrostatic balance between the temperature and thickness fields can be destroyed barotropically as well as baroclinically. In order to recover these balances, intense secondary circulations are generated and very strong upward vertical motions are excited. Usually there exists a plentiful supply of moisture from the southerlies in the low

troposphere, and so the very strong potential instability in the lower troposphere over that area can be released. Vigorous condensation and severe precipitation are then produced.

Torrential rain resulting from vortex/shear-line systems has been one of the most popular subjects of synoptic investigations in China since the 1950's. Some statistical results have been summarized by Lo (see Yeh and Gao, 1979). He also suggested that horizontal convergence in the lower troposphere must be the main dynamic factor for the formation of vortices, and the release of potential instability must be the main thermodynamic factor for their development. The Lasah Workshop of Meteorological Scientific Research on the QTP (1981) recently made a thorough synoptic and climatic investigation of the formation, development and movement of such systems. They showed that in July vortices usually develop in saddle fields at 500 mb, with the Iran High to the west, WPSH to the east, westerly trough to the north, and the easterly trough (the so called reversed trough) to the south. At 100 mb, when the Southern Asian High (SAH) is located between 76°E and 100°E, the divergence of the wind field on its eastern side is then over the centre of convergence of the saddle field at 500 mb, and this creates a suitable environment for vortices to develop. The latent heat released by the associated flows warms up the air column so that the hydrostatic balance is destroyed. The resulting baroclinic adaptation in turn intensifies the vertical motion. Further release of latent heat is therefore produced. It seems that the large-scale environment has the role of triggering the positive feedback between the vertical motion and condensation. Recent experiments by Dell'Osso and Chen (1984) show that latent heat is extremely important for the genesis of vortices and shear-lines over the QTP, whilst the surface sensible heat fluxes appear to have a damping effect on those systems. Other

experiments (Chen and Dell'Osso, 1984) show that, compared to a dry case, the release of latent heat enhances the vertical motion by a factor of about six over the rainfall area. This intensifies the meridional monsoon circulation over the QTP which thereby strengthens the monsoon low-level jet (LLJ) in the lower troposphere and the easterly jet in the upper troposphere.

Our present study aims at the understanding of the role of mechanical forcing in the genesis of a mesoscale vortex which occurred over the eastern flank of the QTP. In section 2, the observed and analysed data stored at the ECMWF are used to investigate the large-scale environment necessary for the development of this system. In the following section there is a description of a series of numerical experiments carried out with the ECMWF N48 limited area gridpoint model to evaluate different orography schemes and to investigate the influence on the formation of the vortex of the deflected and climbing flows due to the mechanical forcing of the QTP. The ability of the model with either a mean or envelope orography to predict the genesis of the vortex and the consequent torrential rain is exhibited; the effect on the predicted location of the system is also considered. By examining the observed elevation of the QTP, in section 4, a modified orography is then designed in an effort to improve the prediction. The sensitivity of the location of the mesoscale vortex to the local feature of mountains is also investigated. Some discussions and concluding remarks are then given in section 5.

2. SYNOPTIC DESCRIPTION

From 28 to 30 July 1982, a mesoscale- vortex was generated over the eastern flank of the QTP, resulting in torrential rain over a 300X400 km^2 area with the heaviest rainfall of more than 100 mm in one day (Fig. 1). The vortex

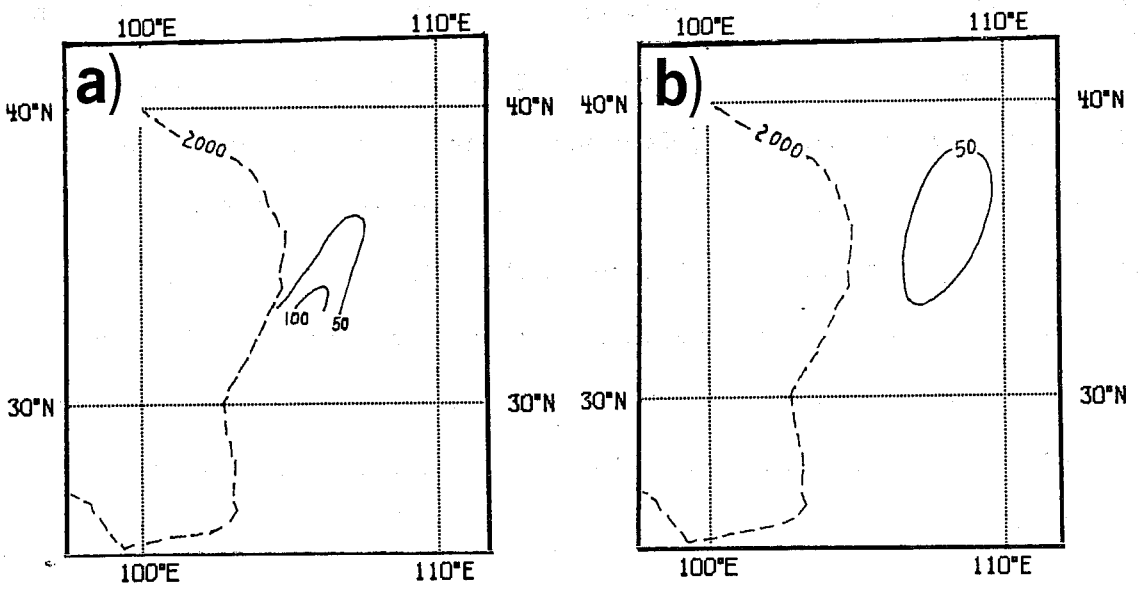

Fig. 1 The distribution of 24 hour rainfall over the eastern flank of the QTP. Units in mm. The dashed line shows the 2 km contour of the plateau.
(a) 00Z 28 to 00Z 29, July 1982 ;
(b) 00Z 29 to 00Z 30, July 1982.

occurred after the circulation over Asia had undergone a marked adjustment which then produced a suitable situation for its development. The synoptic evolution in the stratosphere and troposphere are illustrated by the 100 mb (Fig. 2) and 500 mb (Fig. 3) analyses for 12GMT, 24, 26 and 28 July. Before the 24th, the mid-latitude tropospheric pertubations were rather weak. At 100 mb, the main summer anticyclone was located over the Middle East, south of the Caspian Sea (Fig. 2a). After a sudden increase of the meridional index in the troposphere over Europe on the 24th (see Fig. 3a), the anticyclone at 100 mb moved gradually eastwards and then settled down at about 77°E after the 26th. By this time it had become a stable SAH and provided a favourable environment for the development of vortices (Figs. 2b and 2c).

In the troposphere (Fig. 3), due to the development of a ridge over Europe, the existing weak westerlies in the mid-latitudes over the Eurasian continent were also disturbed after the 24th. Small perturbations in both temperature and geopotential fields propagated eastwards along the weak westerlies over Asia (Fig. 3b). After going around the northern boundary of the QTP on the 28th, the temperature perturbation extended southwards, reaching subtropical latitudes. A vortex with the subsequent torrential rain soon formed (Fig. 3c).

The 500 mb wind reports (Fig. 4) show that before the cold air from the north arrived at low latitudes there had been prevailing southwesterlies associated with the WPSH over the eastern flank of the QTP along 30°N (Figs. 4a and 4b). From the 28th, the northerlies behind the trough in the westerlies started to merge with the existing southwesterlies; a complete vortex was then generated to the west of the WPSH at 31°N, 108°E (Figs. 4c and 3c). At 700 mb

(Fig. 5), the deflected flow on the southern side of the QTP skirted the southeastern corner of the plateau and turned northwards (Fig. 5a). It then met the easterlies associated with the WPSH and formed a shear-line at about 31°N between 104°Eand 114°E (Fig. 5b). The vortex was later produced on this shear-line (Fig. 5c). Moisture was transported to the area by the southwesterlies from the Bay of Bengal and by the easterlies from the East China Sea.

The analysis of cross-sections close to the vortex centre (Fig. 6) illustrates the development of the vortex. Initially (Fig. 6a) the vortex was excited in the low troposphere with a vertical vortex-axis (the zero isotach) at about 106°E. The northerlies on its western flank were weaker than the southerlies to the east. Twelve hours later, as the vortex extended to the upper troposphere, the "vortex chimney" is observed (Fig. 6b) and torrential rain occurred. During this period the southerlies weakened and the northerlies became stronger as a result of the southward advection of the mid-latitude trough. The warm core due to the release of latent heat in the upper chimney then became apparent, and this continued to develop. After a further 12 hours, the vortex became asymmetrical and tilted westwards (Fig.6c). The lower and the western parts of the vortex were cooled, whereas the upper and the eastern parts were warmed. From 00Z 28 to 00Z 29, the 312 K isotherm of the potential temperature was lifted up about 30 mb in the west and moved down about 60 mb in the east. The warm core of the upper vortex also intensified.

3. NUMERICAL EXPERIMENTS

The ECMWF N48 limited area gridpoint model (Burrige and Haseler, 1977) was used for our numerical experiments. There are 15-levels in the vertical with a gridlength of 1.875° in both longitude and latitude. The parameterisation of physical processes, including radiation, condensation, and subgrid scale physics (Tiedtke et al., 1979) is kept unchanged throughout all experiments.

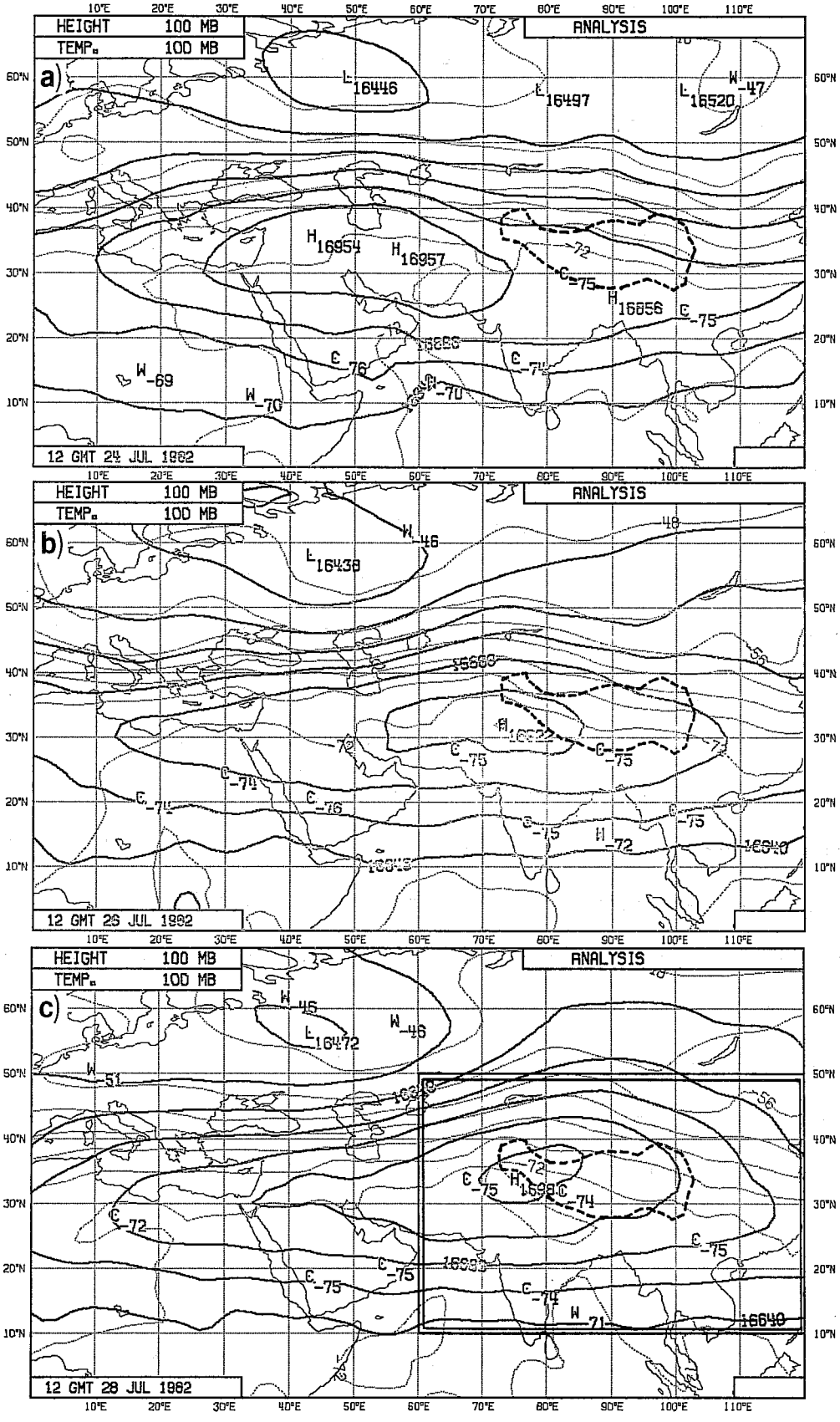

Fig. 2 The analysed successive development of the geopotential (solid lines) and temperature (dotted lines) fields at 100 mb in July 1982. The heavy dashed line shows the 3 km contour of the QTP. The double solid lines in (c) denote the area of verifications for 48-hour forecasts in the following experiments.
(a) 12Z 24 July ; (b) 12Z 26 July ; (c) 12Z 28 July.

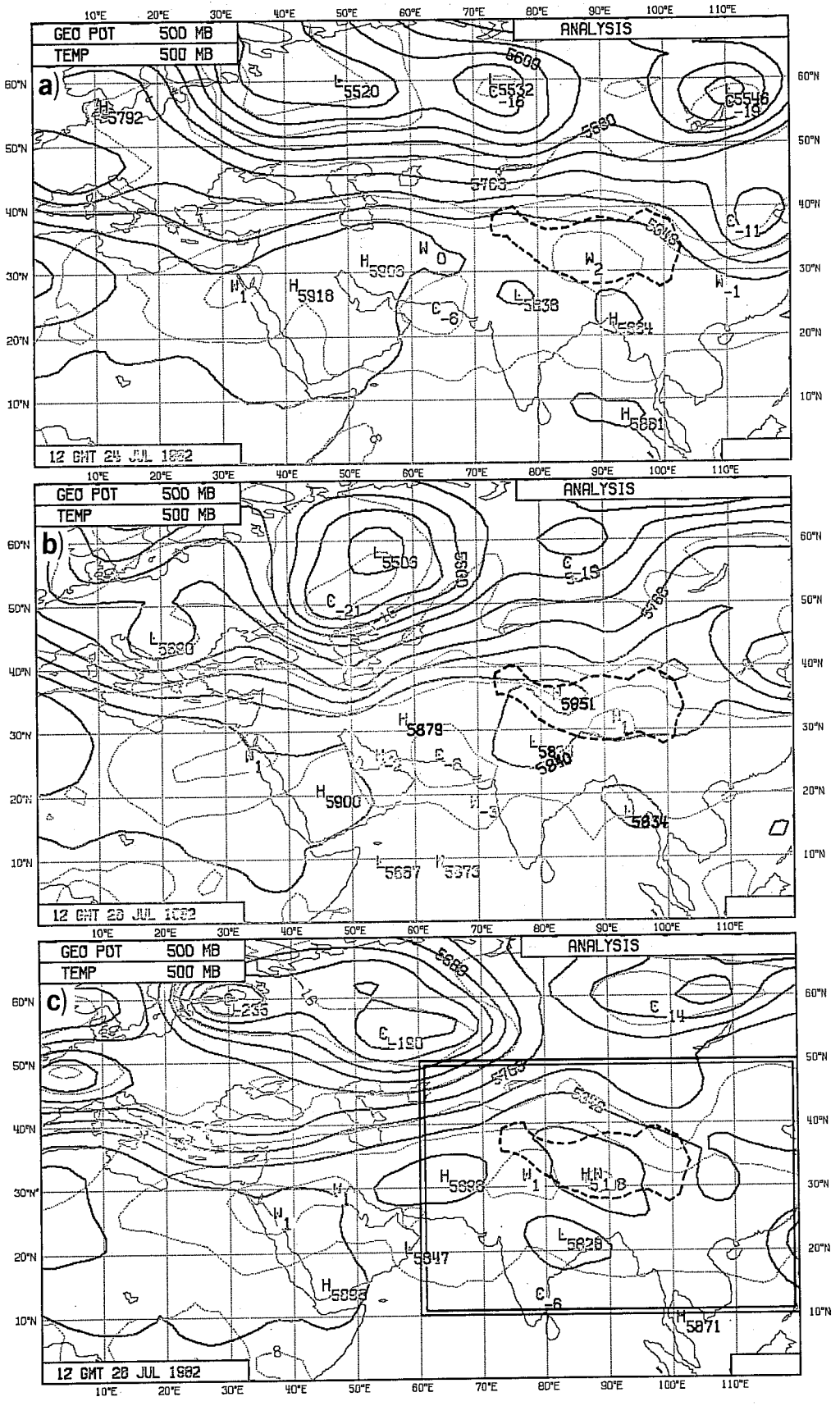

Fig. 3 The same as in Fig. 2, except for 500 mb.

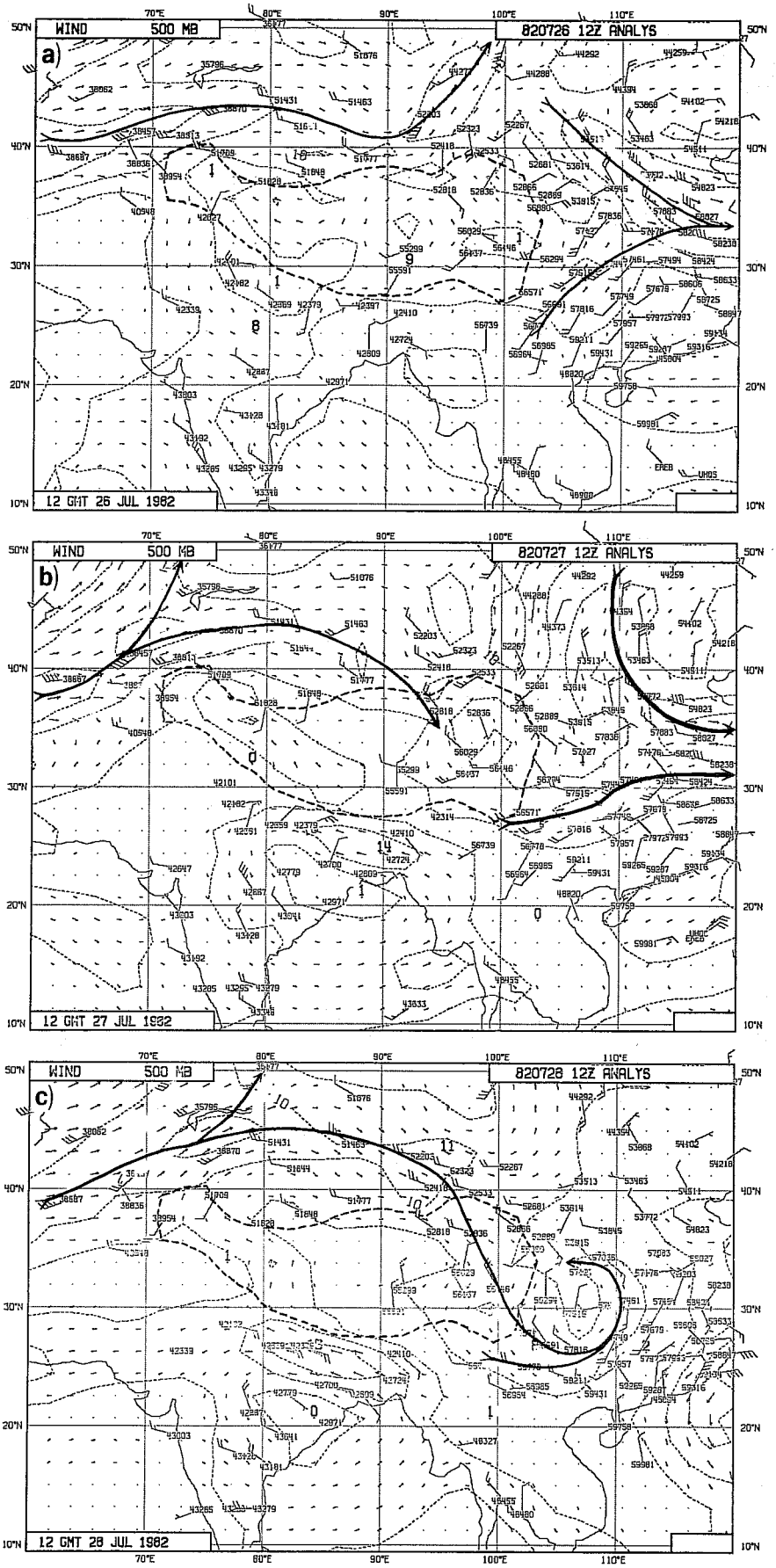

Fig. 4 The analysed successive development of the wind fields on 500 mb in July 1982. Dashed lines are isotachs. Heavy solid lines show the flows connected with the vortex. (a) 12Z 26 July ; (b) 12Z 27 July ; (c) 12Z 28 July.

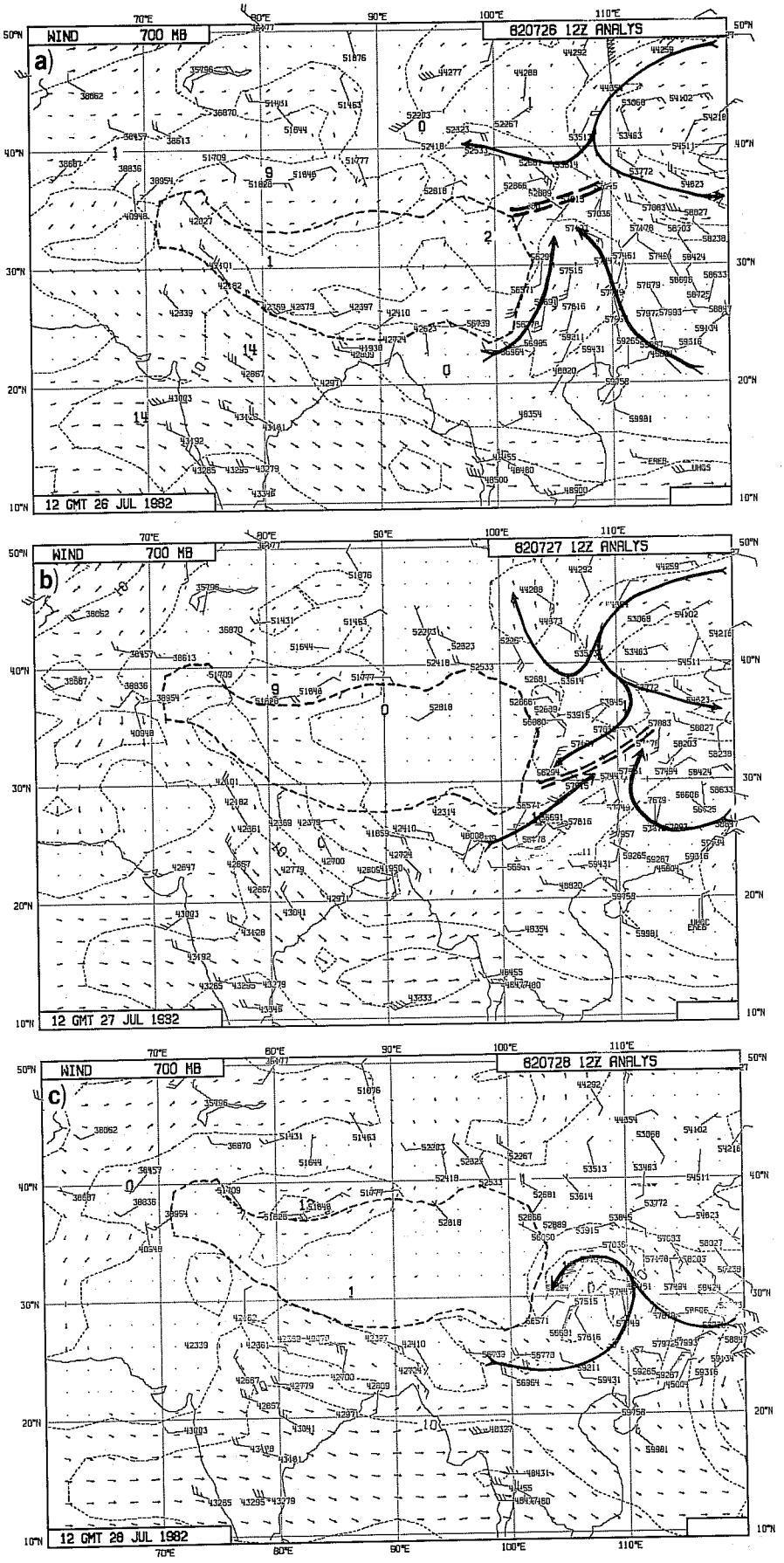

Fig. 5 The same as in Fig. 4 except for 700 mb.

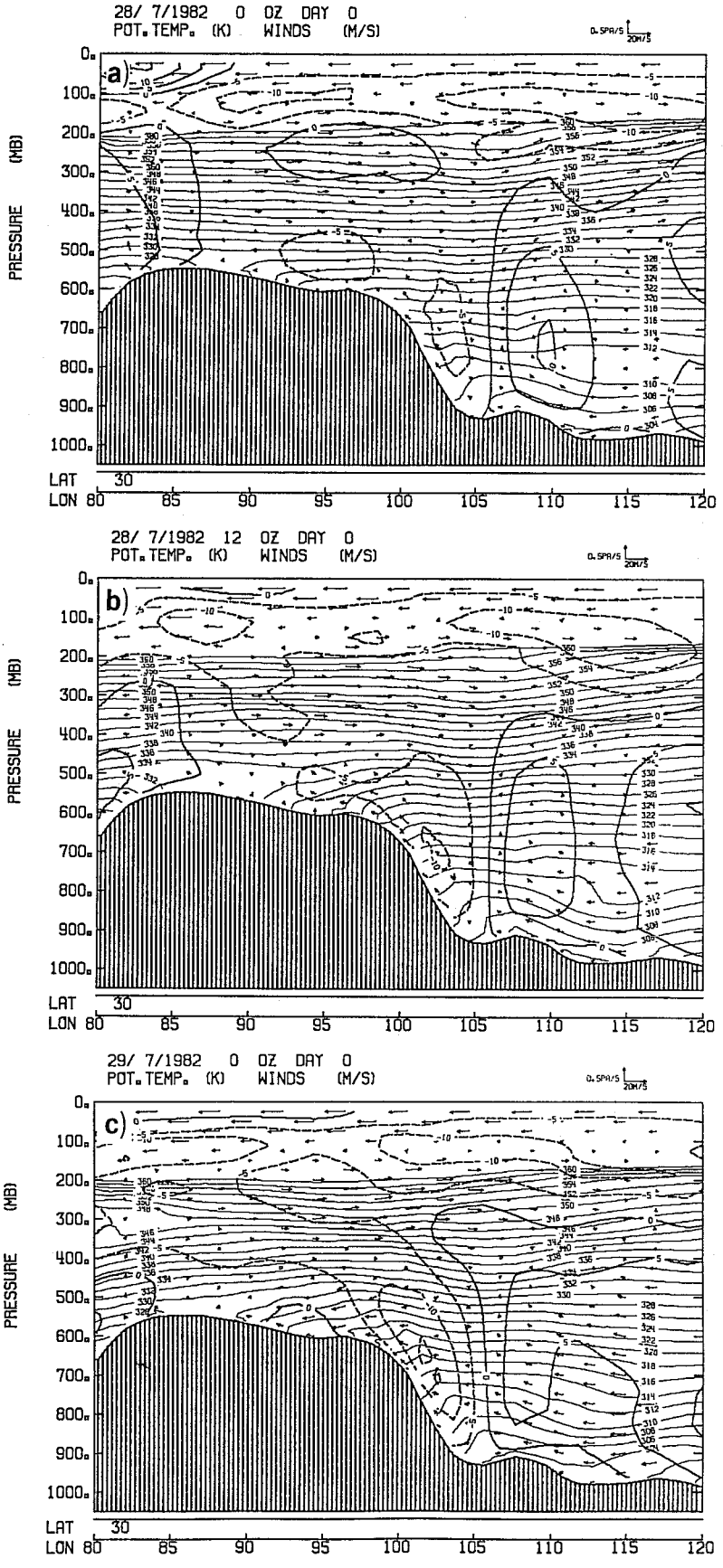

Fig. 6 The cross-section along 30°N produced from analysed data, showing the development of the vortex at about 106° E in July 1982.
(a) OOZ 28 July ; (b) 12Z 28 July ;
(c) OOZ 29 July.

The integration area is bounded from 22.5°W to 160°E, and from the equator to 71.25°N. Boundary values required for time integrations are obtained from analysed data. Whenever an orography is used other than that is the control run, the initialisation is accomplished by allowing the control orography to grow into the new one in the first 12 hours. This procedure may lead to a bias towards the control run in the short term forecasts, but it is expected that this will not be significant for the 48 hour forecasts. Therefore in this investigation only the 48 hour forecasts are evaluated. All the experiments are started from 12Z 26 July, 1982.

3.1 Smoothed orography - the control run (CON)

The orography used in the operational model at the time of our experiments (July, 1982) was the version described by (Tibaldi and Geleyn, 1981) - hereafter referred to as the mean orography. This was derived from the U.S. Navy data which has a resolution of 10' of arc. Also, a gridpoint filter was passed over all grid points using a bi-dimensional normalised Gaussian weighting function with a radius of influence of 100 km.

Fig. 7a shows the QTP using this scheme. The predicted 100 mb and 500 mb contours after 48 hours are shown in Figs. 8a and 8b. Comparison with Fig. 2c and Fig. 3c respectively shows a very good agreement between the predictions and observations. The positions of the SAH at 100 mb and the planetary frontal zone at 500 mb are predicted correctly. Also, as observed the cold trough propagating along this frontal zone reached the northeastern flank of the QTP on the 28th, then suddenly extended southwards; the northerlies behind the trough then merged with the existing southwesterlies to form a vortex (Fig. 8c). The currents associated with the monsoon

low-level jet (LLT) which flowed around the southern and southeastern flank of the QTP at 700 mb are also simulated quite well (Fig. 8d). The mesoscale-α vortex at both 700 mb and 500 mb is formed, and this resulted in torrential rain with a maximum precipitation of 59 mm in 24 hours over that area (Fig. 8e).

The main errors in the prediction are observed in the tropical areas. At 500 mb, the observed Indian low (Fig. 3c) disappears; instead, a strong Indo-China low is predicted at both 500 mb and 700 mb. Also the coarse N48 model fails to predict the observed typhoon at about 22°N, 122°E. All these result in much stronger southerlies towards the vortex at both 500 mb and 700 mb in the predictions.

In sigma coordinates, the budget equation of kinetic energy K can be written in flux form for a unit area of air (Savijarvi, 1981) as

$$\frac{\partial}{\partial t}\left(\frac{p_s K}{g}\right) = R_K - \nabla_\sigma \cdot \left(\frac{p_s}{g} K\underline{V}\right) - \frac{\partial}{\partial \sigma}\left(\frac{p_s}{g} K\dot{\sigma}\right) - \frac{p_s}{g}\underline{V} \cdot \left(\nabla_\sigma \phi + RT\nabla_\sigma \ell n p_s\right)$$

These terms describe the local change, source (denoted as "residual" in Fig. 9a), horizontal flux convergence, vertical flux convergence, and generation (denoted as "conversion" in Fig. 9a) of kinetic energy respectively. The selected area for our calculation ranges from 96° to 112°E, and from 27° to 39°N, as the predicted vortex at 500 mb in the CON-case lies in this region. Numerical outputs from the 24 to 48 hour forecasts are taken for the calculation, and the results are shown in Fig. 9. There are several interesting features.

(a) There are two maxima of kinetic energy generation located at 200 mb and 700 mb respectively. The maximum near the surface results from the low level inflow towards the centre of the vortex (Fig. 8d), and the maximum at

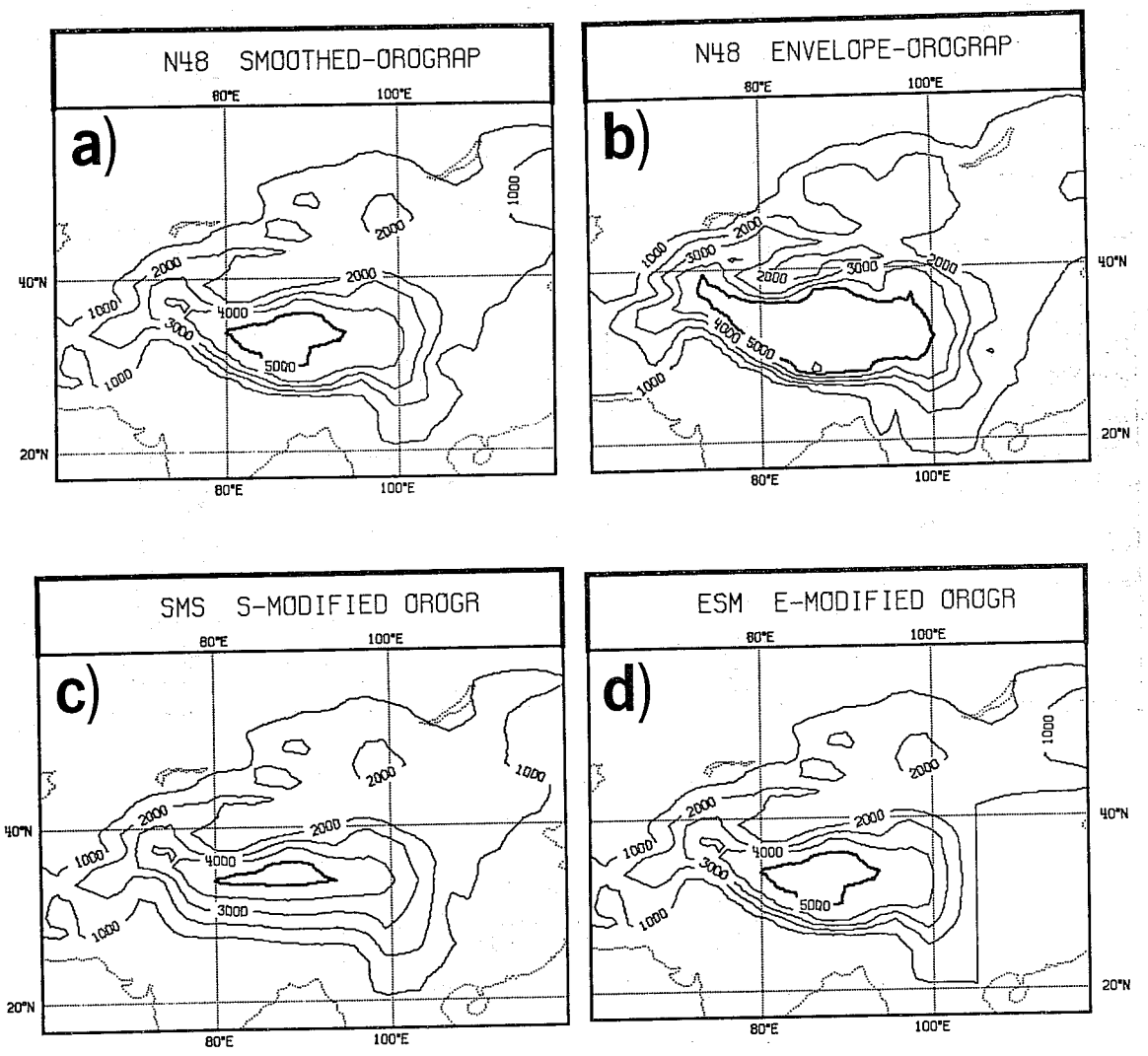

Fig. 7 The QTP under different orography schemes in our experiments.

(a) The mean scheme in the control run CON;

(b) The envelope scheme in the run ENV ;

(c) The orography with a smoothed southern flank in the run SSM (see text for detail).

(d) the orography with its eastern slope modified in the experiment ESM (see text for detail).

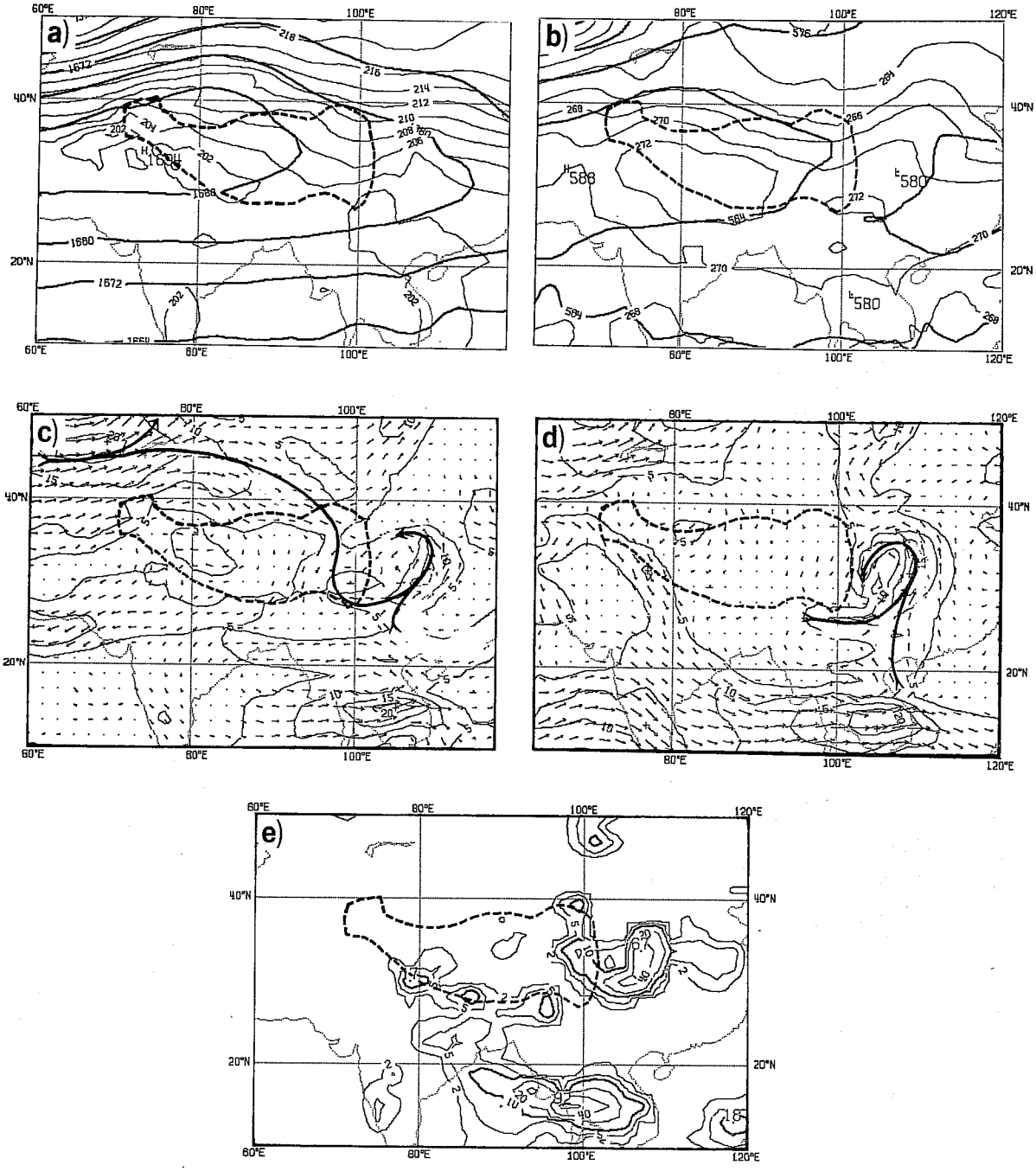

Fig. 8 The 48-hour predictions from the experiment CON with the mean orography. The heavy dashed line shows the 3 km contour of the QTP under this scheme.

(a) Geopotential and tmeperature fields at 100 mb.

(b) Geopotential and temperature fields at 500 mb.

(c) Wind fields at 500 mb.

(d) Wind fields at 700 mb.

(e) The 24 hour accumulated precipitation between T+24 and T+48.

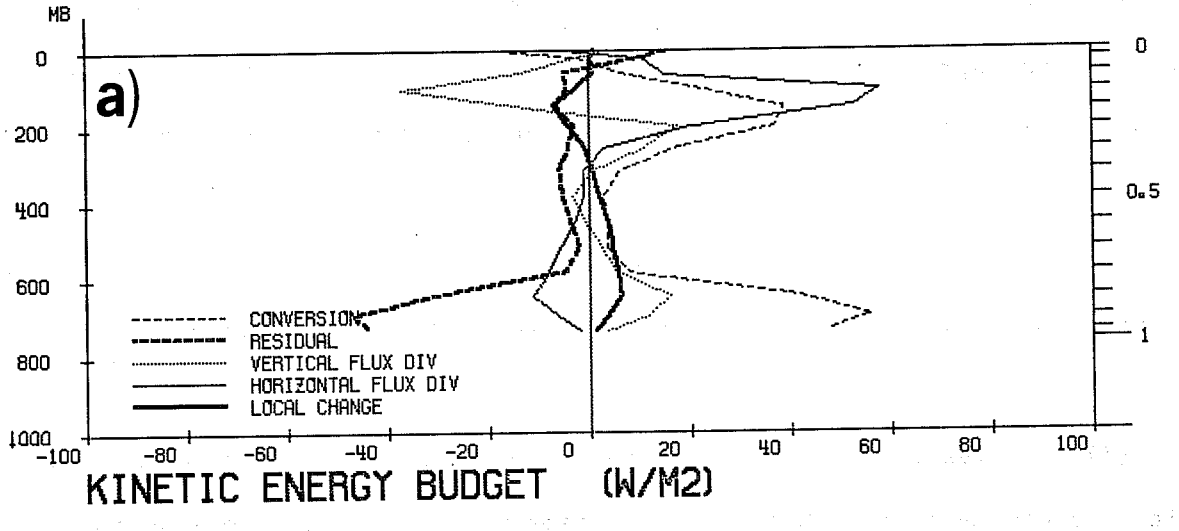

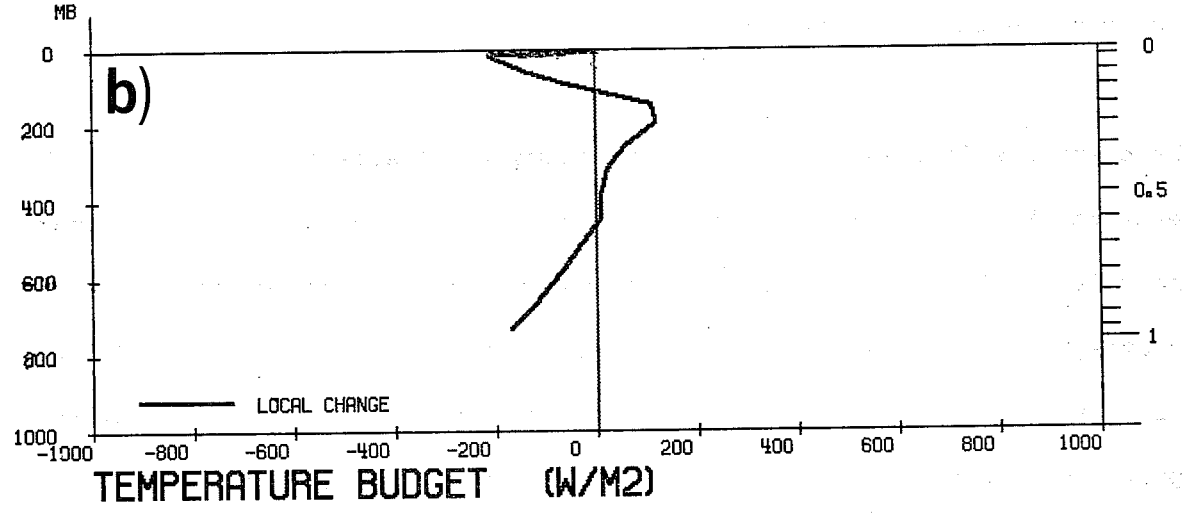

Fig. 9 (a) The vertical distribution of the kinetic energy budget, and (b) the local change of sensible heat $\partial(P_s C_p T/g)\partial t$, of the vortex in the experiment CON with mean orography.

upper level implies that there are subgeostrophic winds there. This generation is mostly balanced by frictional dissipation at levels below 600 mb, and by horizontal divergence of energy flux near the tropopause.

(b) Below 300 mb, kinetic energy is transported towards the vortex but in the stratosphere it is strongly transported out of the area. The maximum at 700 mb should be attributed to the strong low level inflow into the vortex.

(c) Below 300 mb, the kinetic energy of the vortex has increased, whereas above this level the kinetic energy over this area is decreased.

(d) The vertical flux of K in the troposphere is positive everywhere, with two maxima at 500 mb and 200 mb respectively. Kinetic energy is therefore strongly transferred from the low to the high troposphere and from the troposphere to the stratosphere.

The overall effect is that the vortex chimney collects the converged and generated kinetic energy at low levels and transports them to high levels, and this results in an intense horizontal output of kinetic energy in the stratosphere over the same area. At the same time the low levels of the vortex are cooled due to the invasion of cold air from the north, whereas the upper layer is warmed by the release of latent heat (Fig. 9b).

3.2 Envelope orography experiment (ENV)

Wallace et al. (1983) found that an underestimation of orographic forcing, via the lower boundary conditions of the model (the mean orography), can result in systematic errors in numerical weather forecasts. To overcome this

problem an envelope orography was then produced in which the terrain height h at each N48 gridpoint is given by

$$h = \bar{h} + \sqrt{2}\,\sigma$$

where $\bar{h}$ is the mean height, and σ is the standard deviation.

As with the mean orography, the envelope orography is derived from the United States Navy data set. The orography of the QTP using this scheme is shown in Fig. 7b. The envelope orography has been shown to give some improvements in the forecasts of large-scale systems, especially over a medium range period and in the upper layers of the model in winter.

Our present interest concerns whether this scheme can predict a mesoscale vortex occurring mainly in the low and middle troposphere. Fig. 10 shows some results from the 48 hour prediction. Overall the geopotential and temperature fields at 100 mb and 500 mb (Fig. 10a and Fig. 10b) are very similar to those from the smoothed scheme (Fig. 8a and 8b) and from the observations (Figs. 2c and 3c). Despite the differences between the experiment and the observations concerning about the inflow structure and the location, the vortex is also generated in the lower troposphere (Figs. 10c and 10d) with 93 mm rainfall in 24 hours (Fig. 10e). It seems that the N48 gridpoint model with either the mean or the envelope orography is capable of predicting such mesoscale systems.

In addition to the prediction errors in the tropics using the mean scheme, some errors in the subtropical and middle latitude areas using the envelope scheme are also observed. The 48 hour predictions using the envelope orography erroneously possess a trough along 120°E in the upper

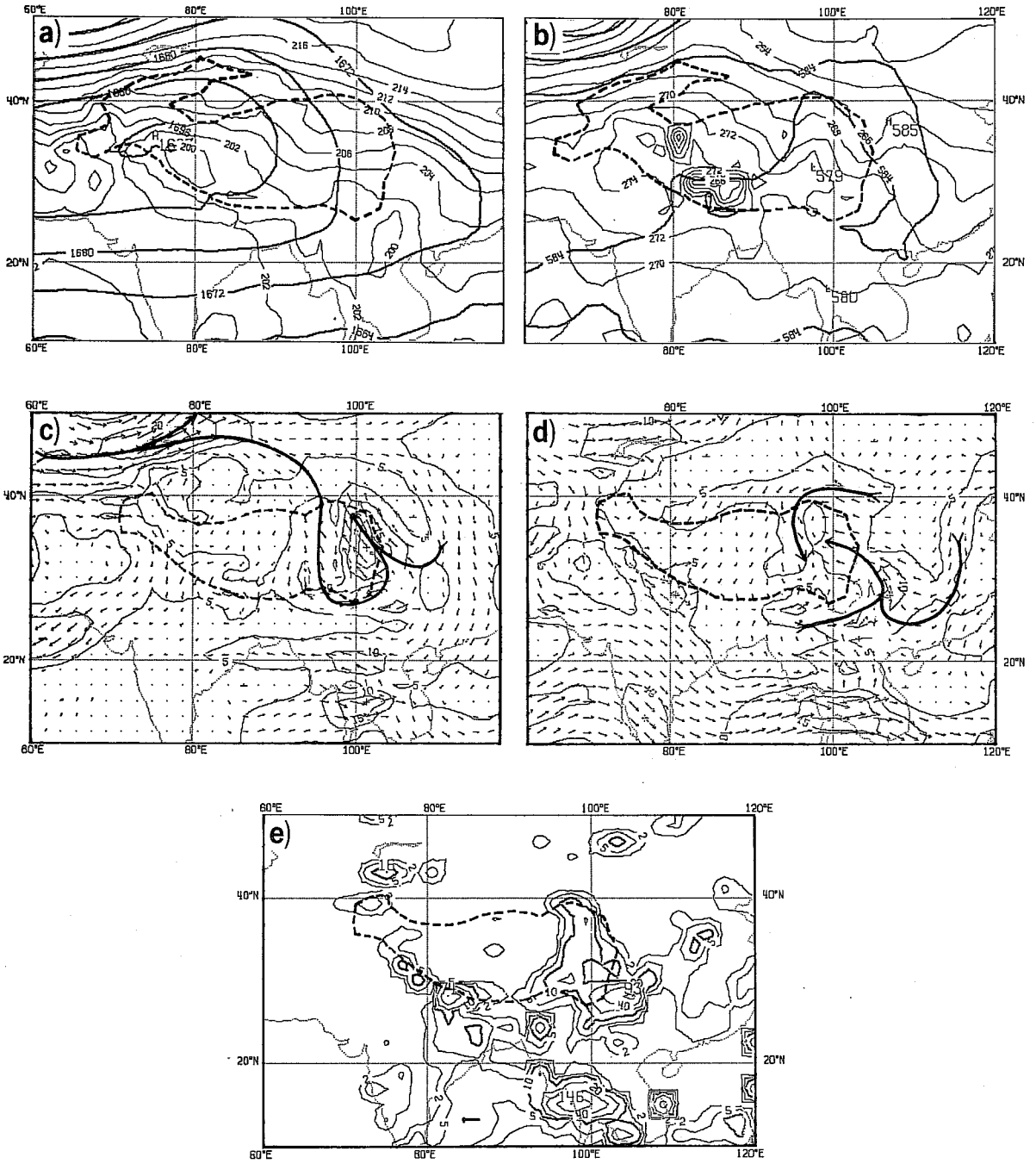

Fig. 10 The experimental results from ENV. The heavy dashed line shows the 3 km contour of the envelope orography. See Fig. 8 for captions.

troposphere and lower stratosphere between 20°N and 45°N. At 500 mb, between this trough and the predicted vortex, there exists a "high pressure dam" at about 108°E. The northerlies between 110° and 120°E hence become rather strong and penetrate southwards towards subtropical areas. Some parts of this flow turn westwards to form the vortex. In comparison with the analyses (Fig. 5c), an extra northerly flow towards the vortex at 700 mb is also observed.

3.3 The effects of mechanical forcing on the formation of the vortex

The main discrepancy between the observations and forecasts shown above is the location of the vortex: in both forecasts it is generated too far west towards the inner area of the plateau. Although the envelope scheme seems to be good for systems in the upper layers of the model, it is even worse than the mean scheme in producing the vortex. This deserves further consideration.

Theoretically, the effect of large scale mechanical forcing in the presence of friction is to generate a geopotential ridge on the windward side and trough on the lee side of a mountain in the westerlies, either barotropically or baroclinically. Also there exists a critical mountain height H_c of about 1-2 kms; for mountains lower than H_c, the climbing effect of flows is dominant, and for mountains higher than H_c, the deflecting effect becomes more important (Wu, 1984). The height of the Himalayas is about 5300 m in the smoothed scheme and 7000 m in the envelope scheme. Low level air flows impinging upon such a huge mountain range are split or deflected as observed in Figs. 3, 4, 8, and 10, whereas middle layer flows approching the QTP may climb or go around the obstacle. Experiments were designed to investigate the different mechanical effects on different branches of the flow. In the

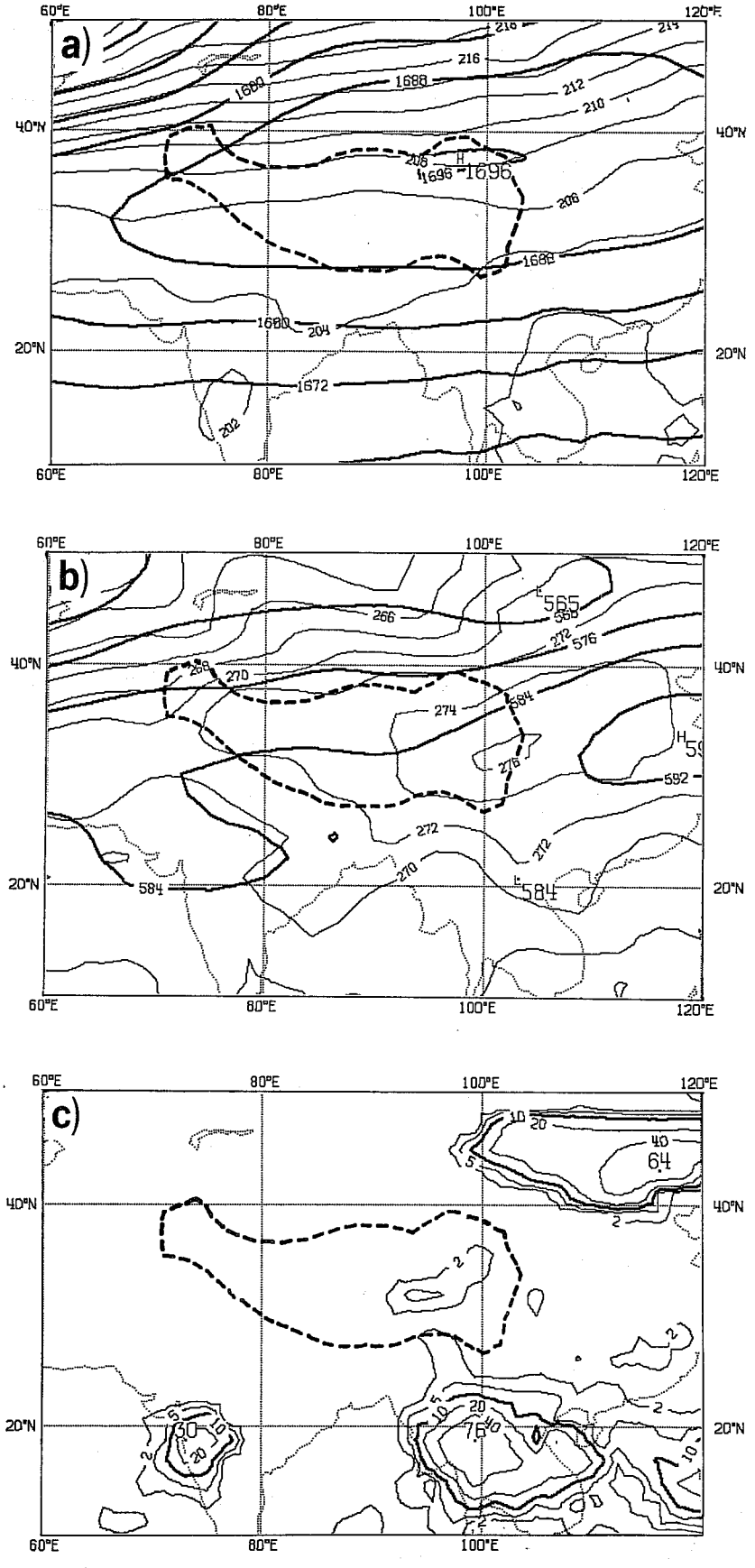

Fig. 11 The experimental results from the case NOM without orography. See Fig. 8 for captions.

first experiment (NOM - no mountain) the mountains are totally removed. The second (SSM - southern slope modified) involves making the upper part of the southern slope of the plateau more gentle so as to see how the LLJ is affected. This is achieved by replacing the orography between 70° to 105°E and from 26°N to 34°N by a "cone plane": along every longitude on this plane, the gridpoint elevation is linearly interpolated from the values at 26.25°N and 33.75°N (Fig. 7c). In the third experiment (HAL - mountain height halved) the mountain height is halved in order to investigate the influence of the QTP on the middle latitude jet and the LLJ.

From the first experiment it is found that the absence of the plateau causes the existing middle latitude cold air to rush down to the low latitudes from the west in the region the plateau should have occupied (Fig. 11). Also the disappearence of the mechanism for generating positive vorticity over the eastern flank of the QTP makes the WPSH extend further westwards. A large amplitude pertubation is then created over the plateau which is not observed there. Hence, over the area where the torrential rain occurred, the deformation field is absent, the vortex disappears, and the weather turns out to be extremely dry (Fig. 11c). It is clear that without the mechanical forcing due to the QTP, even the large-scale environment for the generation of the vortex cannot exist. In other words, the deflecting effect of the QTP must play an important role in the formation of the vortex.

Note that the air flow travelling in the south of the QTP is located at 850-700 mb, well below the plateau, but the flow travelling in the north of the QTP, which is associated with the mid-latitude jet, is located more than 3 km above mean sea level. If the deflecting effect due to the QTP is really important, then just changing the upper part of the southern slope of the

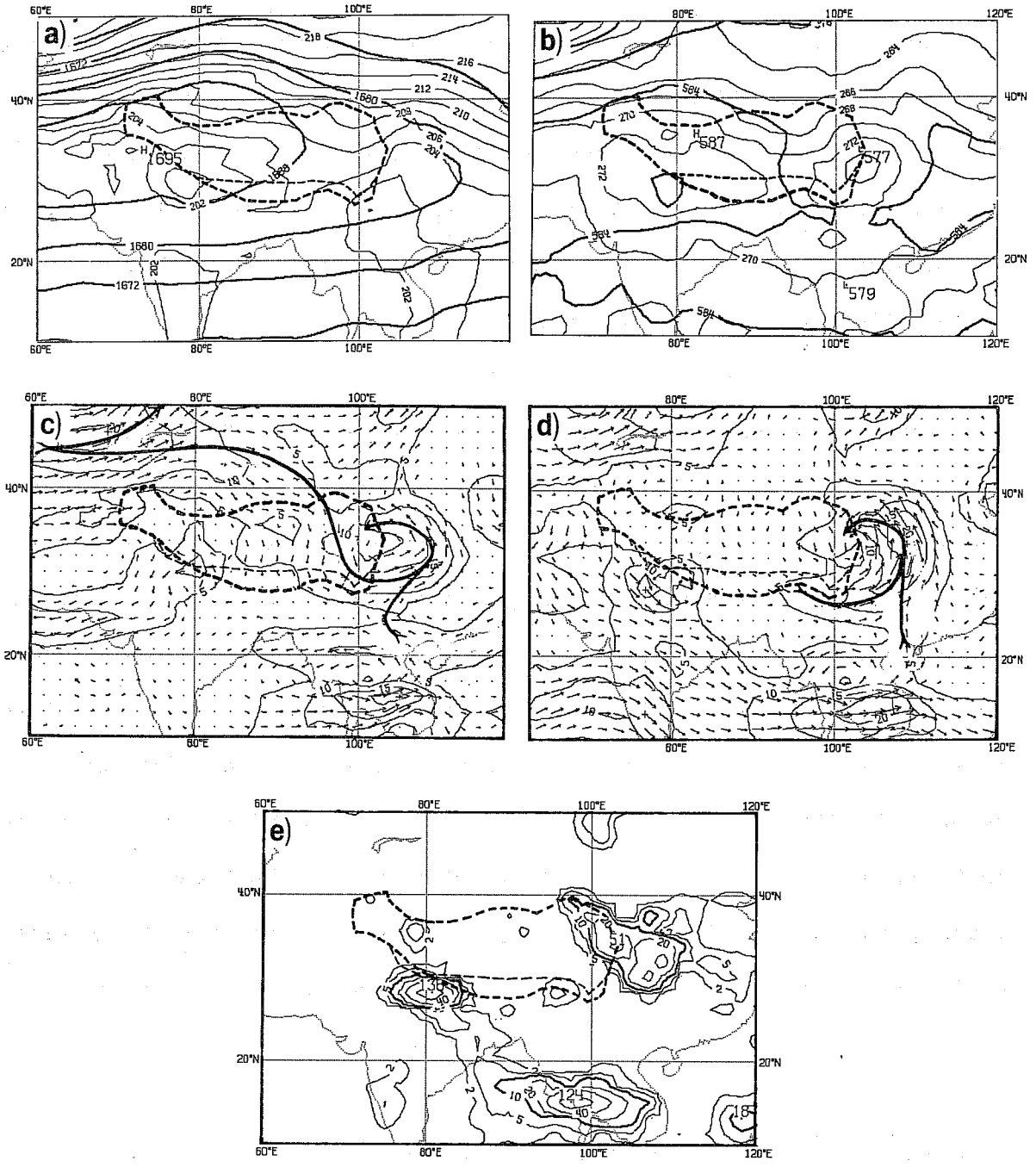

Fig. 12 The experimental results from the case SSM. The light dashed line represents the 3 km contour under this experiment, denoting the modification of the southern slope of the QTP. See Fig. 8 for captions.

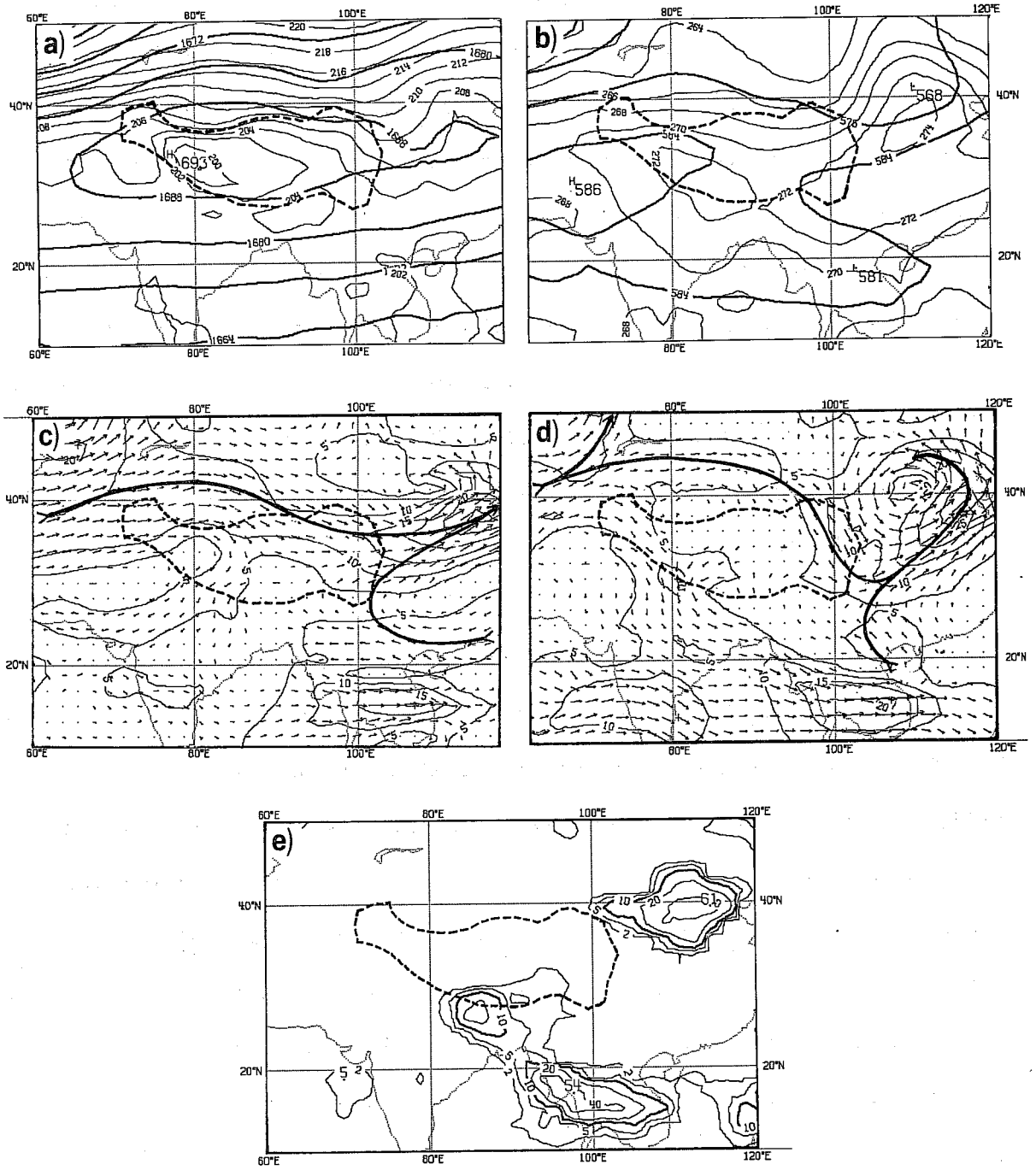

Fig. 13 The experimental results from the case HAL (halving mountain height). The heavy dashed line now denotes the 1.5 km contour of the halved QTP. See Fig. 8 for captions.

plateau, but keeping its height and area unchanged as in the second experiment (SSM), will not cause substantial changes to the prediction. On the other hand, lowering the mountain height, as in the third experiment (HAL), can be expected to generate dramatic changes in the middle latitude flow. These are indeed the results we obtained. In the second case (SSM), the predicted temperature-geopotential structure, the stream field, the vortex at 700 mb and 500 mb, and even the distribution of rainfall etc. (Fig. 12) are all very similar to those in the control run (Fig. 8). However in the third case (HAL), the mid-latitude cold trough climbed up to the top of the lowered plateau, although the flow on the southern side of the QTP does not change very much. Since the Richardson number there is a minimum, a pronounced middle latitude pertubation develops over the prediction period (Fig. 13), and the vortex disappears.

It seems plausible to conclude that the deflecting effect of the QTP plays a fundamental role in the formation of the vortex. Over the eastern flank of the QTP, besides the warm and wet low-level easterlies associated with the WPSH, the warm and wet southern branch of the flow in the lower troposphere moves northwards, while the cold and dry northern branch in the middle troposphere turns southwards. When these three branches meet, the potentially warm air ascends and the potentially cold air descends, so that the pertubation vortex is generated. Torrential rains are usually observed in the eastern parts of vortices. This also supports our reasoning.

There is no doubt that the latent heat release should also play a very important role in the development of the vortex. In fact, in a dry experiment, the intense vortex did not even exist. However this is beyond the scope of the work described here and so we will not discuss it further.

Readers are referred to Dell'Osso and Chen (1984), and Chen and Dell'Osso(1984) for a description of the role of latent heat release.

4. THE MODIFIED OROGRAPHY AND THE EXCITED VORTEX

The excessive smoothing of the orography can cause a substantial reduction of its elevation and results in the weakening of stationary waves mainly in the upper layers of a numerical prediction model. It also seems plausible that such smoothing could contaminate some of the main features of the orography, and thus distort the transient systems in the lower troposphere. Were it true, the westward shifting of the predicted vortex in the case of either smoothed or envelope orography should result from the insufficient representation of local mechanical forcing in the model. Fig. 14 shows the cross-section of the mean as well as the envelope orography along 35°N. Observed elevations of some stations close to this latitude are also shown. We see that the 1000 m contour line has been shifted eastwards by both these orography schemes. This results in a more gentle slope west of 105°E. Since before the vortex was generated there had already been easterlies over the eastern flank of the QTP at 850 mb and 700 mb associated with the WPSH, such a gentle slope might cause the easterlies to reach further westwards, and so result in the westward shifting of the vortex. Hence, the experiment described in this section is conducted in an effort to improve the prediction of the location of the vortex by imposing an artificial slope on the eastern flank of the QTP in the mean scheme.

Since there is an observed "step" structure of the eastern slope of the QTP, its eastern flank in the mean scheme between 20.625°N and 41.25°N is modified as follows in order to make the gradient more realistic. At each latitude, the gridpoint elevation from 99.375°E to 105°E is interpolated

linearly between the values at 99.375°E and 1000 m; and from 105°E to 120°E, the elevation decreases linearly from 1000 m to zero. The resulting orography is shown in Fig. 14 and Fig. 7d, with the steepest slope concentrated to the west of 105°E as observed. The results of the numerical prediction are shown in Fig. 15. Compared to the previous results, Fig. 15 shows some important improvements. For example the position of the vortex has been predicted much closer to that observed. Table 1 compares the location and size of the 500 mb vortex and the 24 hour accumulation of rainfall from different experiments with that observed (ANA). It is noticeable that not only the centre but also the size of the vortex are predicted better in the modified case than in other cases.

TABLE 1 Comparision of the location and size of the vortex between observation (ANA) and forecasts with different orography schemes: ESM- with eastern slope modified; CON- the control run with mean orography; ENV- the run with envelope orography.

	vortex centre Lat.(°N)	Lon.(°E)	vortex location S-N (°N)	W-E (°E)	area (degree^2)	24-hour rainfall(mm)
ANA	31	108	27-33	103-112	54	101
ESM	33	106	28-38	100-111	110	67
CON	33	103	27-39	96-112	192	59
ENV	32	98	26-40	93-106	182	93

The cross-sections along 33°N (the northern border of the observed vortex) for different 48 hour forecasts are shown in Fig. 16. The observed vortex at this latitude is located at 106°E and extends vertically up to 350 mb. All numerical experiments produce a deeper and

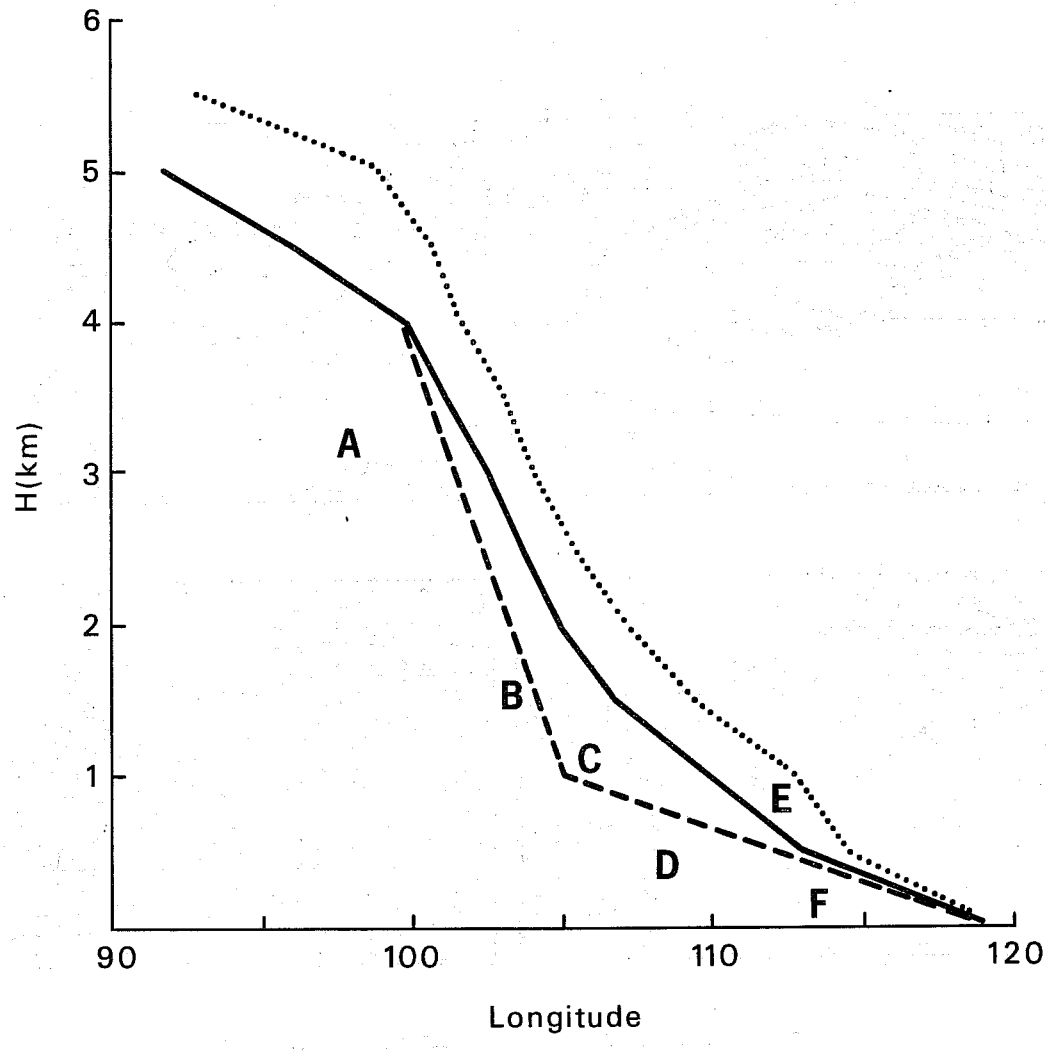

Fig. 14 The eastern slope of the QTP along 35° N using different orographic schemes : dotted line indicates the envelope scheme ; solid line, the mean scheme; dashed line, the modification scheme in the experiment ESM. Letters A-F denote the elevations of some stations close to 35° N.

A: Dulan (36° 20'N, 98° 02'E), 3192 m.

B : Lanzhou (36°03'N, 103°53'E), 1518 m.

C : Yichuan (38°29'N, 106°13'E), 1113 m.

D : Xian (34° 18'N, 108°56'E), 398 m.

E : Taiyuan (37° 47'N, 112° 33'E), 779 m.

F : Zhengzhou (34° 43'N, 113° 39'E), 111 m.

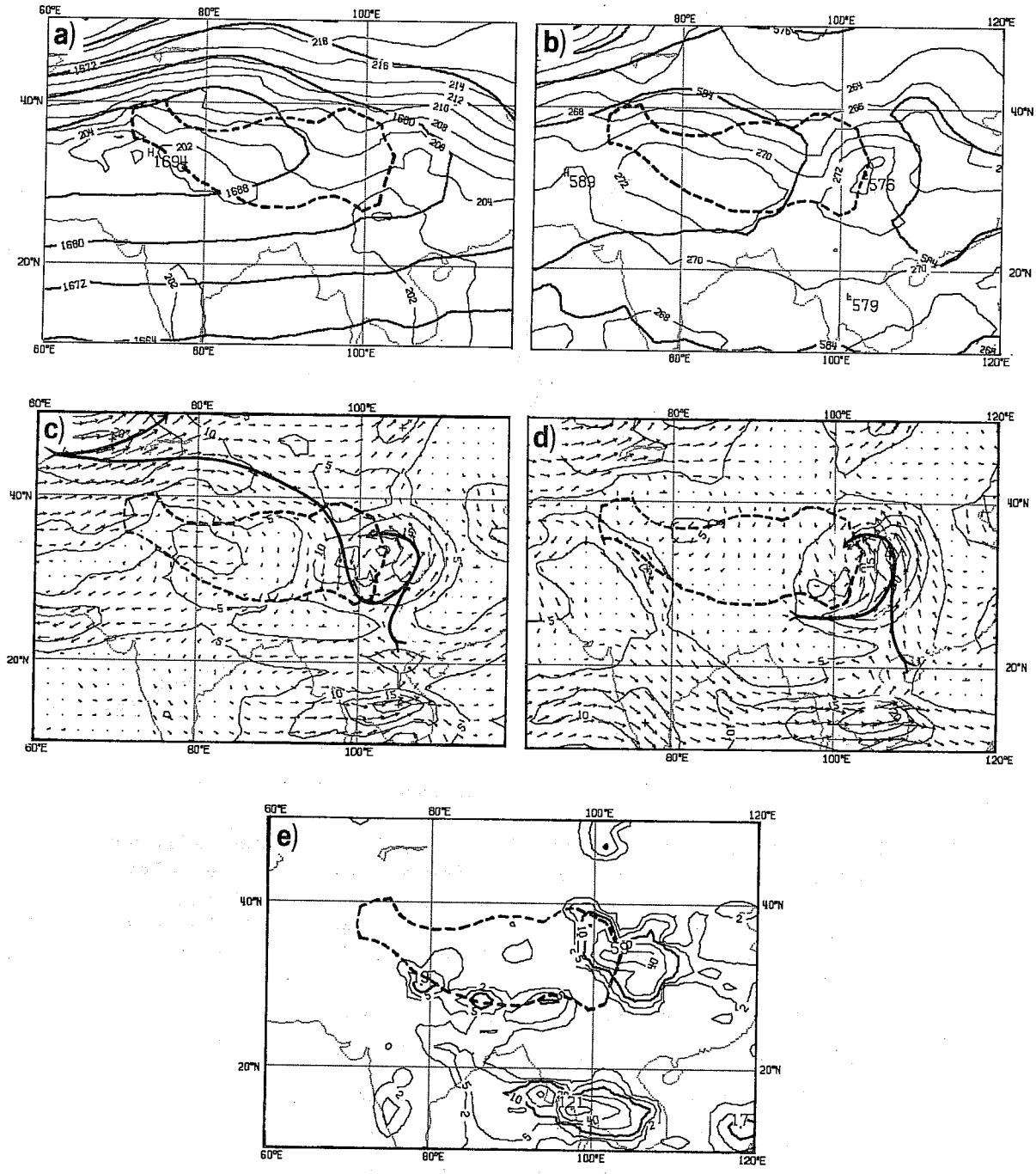

Fig. 15 The experimental results from the run ESM with the eastern slope of the QTP modified. The heavy dashed line denotes the 3 km contour under this scheme. See Fig. 8 for captions.

stronger vortex. However, the observed location, vertical extension, and the "chimney" structure are represented better by the modified orography, and worse by the envelope scheme.

The southeast/northwest cross-section passing through the observed vortex centre (Fig. 17) shows that the northwest part of the vortex is below the tropopause jet. This makes the vortex shallower in the northwest sector and deeper in the southeast sector. We see again that, due to the introduction of the modified orography, the prediction has been improved. In the envelope case, the vortex is not shown since the cross-section only passes through its northeast sector.

Apart from the eastern flank of the QTP, the forecasts in other areas are also improved due to the modification of the orography scheme as shown in the cross-sections along 95°E (Fig. 18) and 40°N (Fig. 19). The improvement of the westerly systems along 40°N under the modified scheme, as shown by Fig. 19, hints that there should be some interactions between the mesoscale vortex and the large-scale systems. Any failure in simulating such mesoscale systems may lead to an inaccurate prediction of large-scale situations.

The overall results from this experiment show that the mesoscale systems around the rugged terrain are sensitive to some of the main features of the orography. Too much smoothing of the orography may spoil the numerical prediction, especially of mesoscale systems in the lower troposphere.

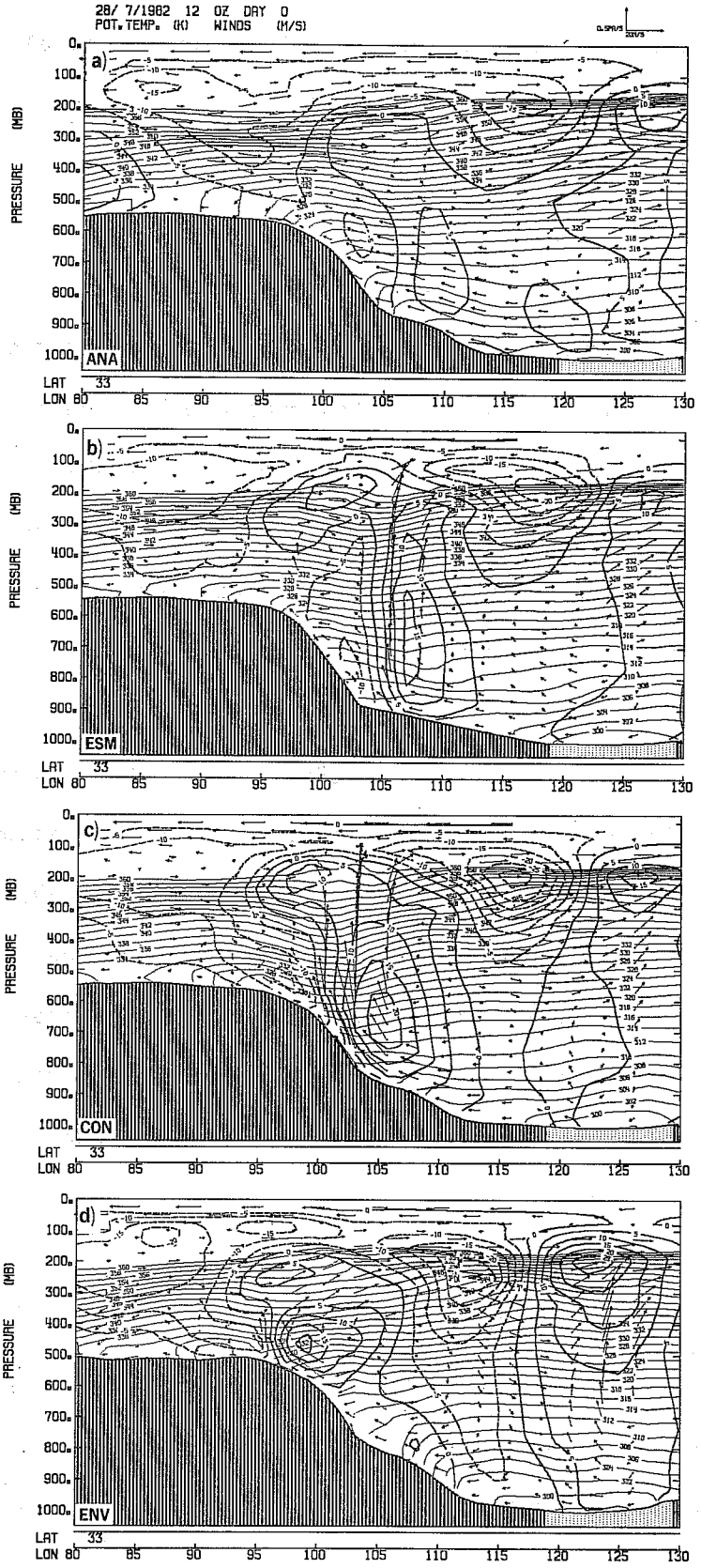

Fig. 16 The cross-sections of the geopotential temperature (light solid lines) and wind fields from different experiments in comparison with the analyses. Heavy solid lines represent the isotaches of southerlies, and heavy dashed lines, of northerlies.
(a) Analyses ; (b) ESM-run ; (c) CON-run ; (d) ENV-run.

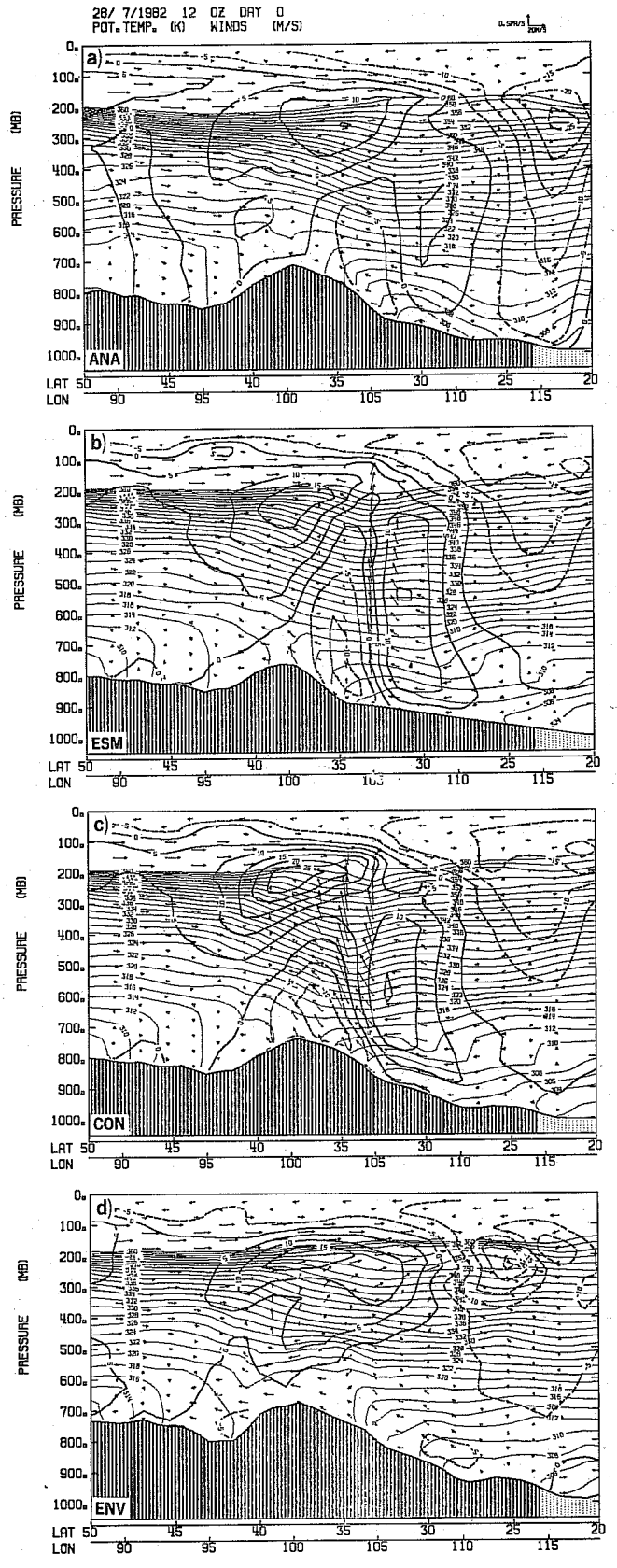

Fig. 17 The northwest-southeast cross-sections passing through the observed vortex centre. Heavy lines denote the isotachs of southwesterlies, and heavy dashed lines, of northeasterlies. See Fig. 16 for captions.

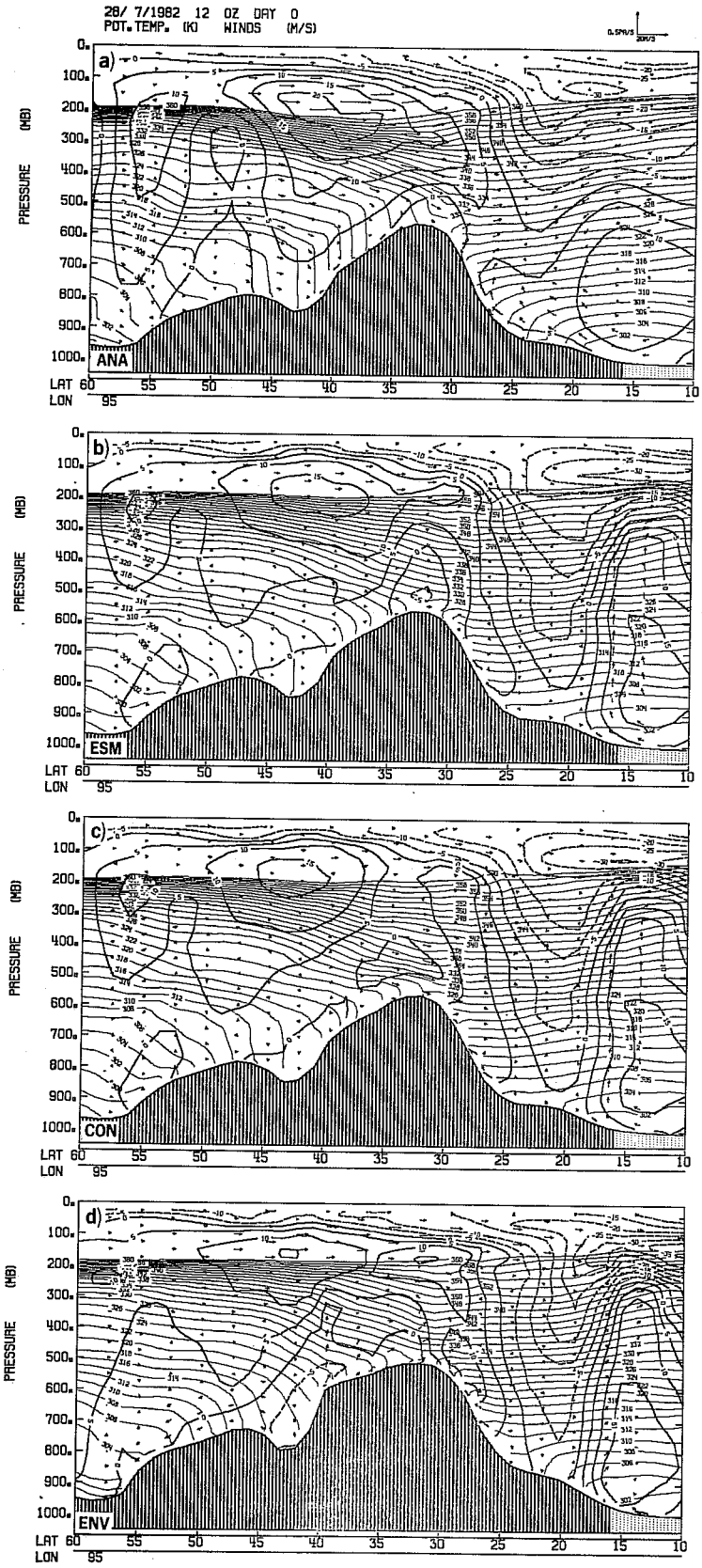

Fig. 18 The cross-sections along 95°E. Heavy solid lines denote the isotaches of westerlies, and heavy dashed lines, of easterlies. See Fig. 16 for captions.

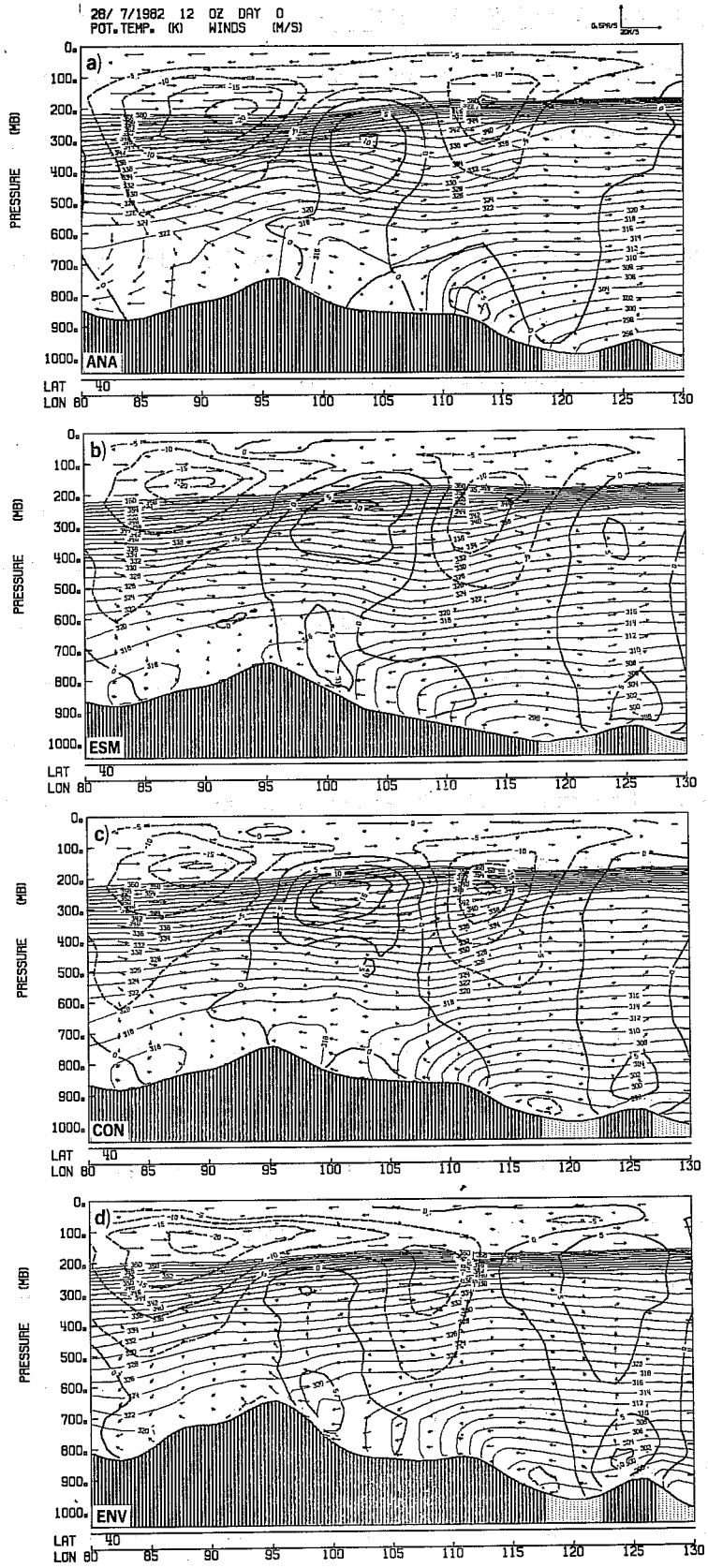

Fig. 19 The cross-sections along 40° N. See Fig. 16 for captions.

5. DISCUSSIONS AND CONCLUDING REMARKS

(a) Excessive smoothing of orography in numerical weather prediction models causes a substantial reduction of elevation and results in less mechanical forcing. Additionally, such smoothing produces much gentler mountain slopes, and results in the distortions in the deflected and climbing flows around the mountains. This can damage the ability of the numerical model to predict mesoscale systems.

(b) In the atmosphere the meridional distribution of mountain torque and frictional torque are similar in sign to one another (Widger, 1949; White, 1949; Newton, 1971b), i.e. positive in extreme latitudes and negative in middle latitudes. Mainly due to thermal effect, the mountain torque of some large mountain complexes, such as the Rockies and the QTP, changes signs in the vertical at about 3 km above mean sea level. But the vertical integration of these mountain torques gives the same sign as that in the lower part of the mountain (Newton, 1971a).

The large scale pressure perturbations in the lower troposphere are mainly due to thermal forcing (Smagorinsky, 1953; Döös, 1962; Wu, 1983). If it is assumed that this forcing does not change appreciably in the numerical experiments in which only the orography is changed, then the lowering of mountain height in the model can result in a spurious source of angular momentum. For example, the excessive smoothing of the QTP in winter will produce a stronger positive mountain torque in subtropical areas. In a quasi-steady state, the spurious positive mountain torque must be balanced by either a decrease of surface easterlies or an increase of divergence of meridional transfer of angular momentum by eddies, thus resulting in stronger zonal flows in middle latitudes. Hence the increase of height of the mountains in the model can result in the reduction of zonal mean kinetic energy. Therefore, the advantage of

replacing the mean orography by the envelope orography in the medium range forecasts is not only to increase the mechanical forcing so as to reduce the systematic errors, but also to give a better representation of the balance of angular momentum, basically due to the increase of mountain height.

(c) The expansion of the mountainous area in the envelope scheme may not necessarily be responsible for the increase of large-scale mechanical forcing, since for such forcing the intensity of the mechanically excited stationary waves depends mainly on the mountain height (Charney and Drazin, 1971; Wu, 1984) in both barotropic and baroclinic situations. On the other hand, as the mountain height is reduced by smoothing, its area is expanded. Then, the further expansion of mountain area by the introduction of the envelope scheme may cause a serious deformation of the surrounding areas of mountains, resulting in increasing error in predicting synoptic systems.

It seems that the introduction of the envelope scheme produces some defects as well as many benefits. Therefore overall improvement may be achieved by modifying the scheme so that it retains some of the merits of the envelope orography whilst alleviating some of its defects. One possible choice is to increase the mountain height in the mean orography but not to expand the mountain area. Another possibility is to use a model with higher horizontal resolution so as to have a more realistic representation of the orography. A new spectral model with much higher resolution is now under construction at ECMWF, and we are looking forward to having a better representation of mechanical forcing in, and more accurate forecasts from, the ECMWF model in the near future.

ACKNOWLEDGEMENTS

All the experiments were carried out on the ECMWF computer system. We would like to thank Dr. S. Tibaldi for helpful discussions and Dr. L. Dell'Osso for his assistance with the limited area model.

We are indebted to Dr R. Riddaway for reading the draft and correcting the grammar.

REFERENCES

Burridge, D.M., and J. Haseler, 1977: A model for medium range weather forecasts - adiabatic formulation. ECMWF Tech.Rep.No.4, 46pp.

Charney, J.G., and P.G. Drazin, 1961: Propagation of planetary-scale disturbances from the lower into the upper atmosphere. J. Geophys. Res., 66, 83-109.

Chen, S.J., and L. Dell'Osso, 1984: Numerical prediction of the heavy rainfall vortex over the eastern Asia monsoon region. ECMWF. (not yet published).

Dell'Osso, L. and S.J. Chen, 1984: Genesis of vortices and shear-lines over the Qinghai-Tibetan Plateau: numerical experiments. ECMWF. Paper presented on the International Symposium on the Tibetan Plateau Mountain Meteorology. May, 1984. Beijing.

Döös, B.R., 1962: The influence of exchange of sensible heat with the earth's surface on the planetary flow. Tellus, 14, 133-147.

Haseler, J. and D.Burridge, 1977: Documentation for the ECMWF grid point model. ECMWF internal report, No. 9, 148pp.

Hoskins, B.J. and D.J. Karoly, 1981: The steady linear response of a spherical atmosphere to thermal and orographic forcing. J. Atmos. Sci., 38, 1179-1196.

Lasah Workshop of Meteorological Scientific Research on the QTP, 1981: On the vortices and shear-lines over the Qinghai-Tebetan Plateau on 500 mb during summer. Science Press, pp. 122. (In Chines).

Newton, C. W., 1971a: Mountain torques in the global angular momentum balance. J.Atmos.Sci., 28, 623-628.

Newton, C. W., 1971b: Global angular momentum balance: earth torques and atmospheric fluxes. J.Atmos.Sci., 28, 1329-1341.

Orlanski, I., 1975: A rational subdivision of scales for atmospheric processes. Bull.Amer.Meteor.Soc., 56, 527-530.

Savijärvi, H., (1981) The energy budgets in North America, North Atlantic and Europe based on ECMWF analyses and forecasts. ECMWF Tech.Rep.No. 27, 33pp.

Smagorinsky, J., 1953: The dynamical influence of large-scale heat sources and sinks on the quasi-stationary mean motions of the atmosphere. Quart.J.Roy. Met.Soc., 79, 342-366.

Tibaldi, S., and J.-F. Geleyn, 1981: The production of a new orography, land-sea mask and associated climatological surface fields for operational purposes. ECMWF Tech.Memo.No.40, pp. 96.

Tiedtke, M., J.-F. Geleyn, A. Hollingsworth, and J.-F. Louis, 1979: ECMWF model, parameterisation of sub-grid scale processes. ECMWF Tech.Rep.No.10, 45pp.

Wallace, J.M., S.Tibaldi, and A.J. Simmons, 1983: Reduction of systematic forecast errors in the ECMWF model through the introduction of an envelope orography. Quart.J.Roy.Met.Soc., 109, 683-718.

Wu, G.X., 1977: On the distribution of physical quantities and the prediction methods of torrential rains occurred to the northeastern flank of the Qinghai-Tibetan Plateau. Symposium of the second national conference on numerical weather prediction. Science Press, pp. 330. (In Chines).

Wu, G.X., 1978: The dynamical and thermodynamical aspects of torrential rain occurred to the northeastern flank of the QTP. Symposiums of 1978. Central Observatory of Lanzhou, 1-31. (In Chinese)

Wu, G.X., 1983: The influence of large-scale orography upon the general circulation of the atmosphere. Ph.D. Thesis. London University, 203pp.

Wu, G.X., 1984: The non-linear response of the atmosphere to large-scale mechanical and thermal forcing. To be published in J.Atmos.Sci.

Yeh, T.C., and Y.X. Gao, 1978: Meteorology of the Qinghai-Tibetan Plateau. Science Press, pp. 278. (In Chinese).

ECMWF PUBLISHED TECHNICAL REPORTS

No.1 A Case Study of a Ten Day Prediction

No.2 The Effect of Arithmetic Precisions on some Meteorological Integrations

No.3 Mixed-Radix Fast Fourier Transforms without Reordering

No.4 A Model for Medium-Range Weather Forecasting - Adiabatic Formulation

No.5 A Study of some Parameterizations of Sub-Grid Processes in a Baroclinic Wave in a Two-Dimensional Model

No.6 The ECMWF Analysis and Data Assimilation Scheme - Analysis of Mass and Wind Fields

No.7 A Ten Day High Resolution Non-Adiabatic Spectral Integration: A Comparative Study

No.8 On the Asymptotic Behaviour of Simple Stochastic-Dynamic Systems

No.9 On Balance Requirements as Initial Conditions

No.10 ECMWF Model - Parameterization of Sub-Grid Processes

No.11 Normal Mode Initialization for a Multi-Level Gridpoint Model

No.12 Data Assimilation Experiments

No.13 Comparisons of Medium Range Forecasts made with two Parameterization Schemes

No.14 On Initial Conditions for Non-Hydrostatic Models

No.15 Adiabatic Formulation and Organization of ECMWF's Spectral Model

No.16 Model Studies of a Developing Boundary Layer over the Ocean

No.17 The Response of a Global Barotropic Model to Forcing by Large-Scale Orography

No.18 Confidence Limits for Verification and Energetic Studies

No.19 A Low Order Barotropic Model on the Sphere with the Orographic and Newtonian Forcing

No.20 A Review of the Normal Mode Initialization Method

No.21 The Adjoint Equation Technique Applied to Meteorological Problems

No.22 The Use of Empirical Methods for Mesoscale Pressure Forecasts

No.23 Comparison of Medium Range Forecasts made with Models using Spectral or Finite Difference Techniques in the Horizontal

No.24 On the Average Errors of an Ensemble of Forecasts

ECMWF PUBLISHED TECHNICAL REPORTS

No.25 On the Atmospheric Factors Affecting the Levantine Sea

No.26 Tropical Influences on Stationary Wave Motion in Middle and High Latitudes

No.27 The Energy Budgets in North America, North Atlantic and Europe Based on ECMWF Analyses and Forecasts

No.28 An Energy and Angular-Momentum Conserving Vertical Finite-Difference Scheme, Hybrid Coordinates, and Medium-Range Weather Prediction

No.29 Orographic Influences on Mediterranean Lee Cyclogenesis and European Blocking in a Global Numerical Model

No.30 Review and Re-assessment of ECNET - a Private Network with Open Architecture

No.31 An Investigation of the Impact at Middle and High Latitudes of Tropical Forecast Errors

No.32 Short and Medium Range Forecast Differences between a Spectral and Grid Point Model. An Extensive Quasi-Operational Comparison

No.33 Numerical Simulations of a Case of Blocking: the Effects of Orography and Land-Sea Contrast

No.34 The Impact of Cloud Track Wind Data on Global Analyses and Medium Range Forecasts

No.35 Energy Budget Calculations at ECMWF: Part I: Analyses

No.36 Operational Verification of ECMWF Forecast Fields and Results for 1980-1981

No.37 High Resolution Experiments with the ECMWF Model: a Case Study

No.38 The Response of the ECMWF Global Model to the El-Nino Anomaly in Extended Range Prediction Experiments

No.39 On the Parameterization of Vertical Diffusion in Large-Scale Atmospheric Models

No.40 Spectral characteristics of the ECMWF Objective Analysis System

No.41 Systematic Errors in the Baroclinic Waves of the ECMWF Model

No.42 On Long Stationary and Transient Atmospheric Waves

No.43 A New Convective Adjustment Scheme

No.44 Numerical Experiments on the Simulation of the 1979 Asian Summer Monsoon

No.45 The Effect of Mechanical Forcing on the Formation of a Mesoscale Vortex